

Letter of Intent

to

Search for Charm and Beauty Particles in  
Proton-Proton Collisions in a FMPS Experiment at the Tevatron †

G. Bellini, S. Bonetti, C. Cerrina-Palazzi, M. Di Corato,  
P.L. Frabetti,\* P.F. Manfredi, D. Menasce, E. Meroni,  
L. Moroni, F. Palombo, F. Ragusa, S. Sala

Istituto di Fisica and Sezione INFN, Milano

F. Bossi, E. Calligarich, C. Castoldi,  
G. Liguori, S. Ratti

Istituto di Fisica Nucleare and Sezione INFN, Pavia

M. Artuso, G. Collins, R. Craven,  
J. Ficenec, S. Mikocki, P. Trower

Virginia Tech

(February 9, 1981)

24 pgs.

## Letter of Intent

to

Search for Charm and Beauty Particles in  
Proton-Proton Collisions in a FMPS Experiment at the Tevatron1. Introduction

A complete understanding of the production and decay of charm/beauty particles is one of the most important current problems in particle physics. The high energy beams on fixed targets which the FNAL Tevatron will offer is a unique opportunity to study particles with lifetimes  $\sim 10^{-12}$ - $10^{-14}$  seconds. Over the past decade techniques using solid state detectors, developed by the Milan group, have been used at CERN. Thus, we propose here to study the open production of charm/beauty in mesons and baryons using a proton beam in the Fermilab Multiparticle Spectrometer (FMPS).

2. Charm Search

To study hadroproduction of open charm, we will use a Segmented Silicon Detector (SSD) which consists of ~~four~~ forty totally depleted silicon wafers assembled in a telescope with a spacing smaller than  $\sim 100 \mu\text{m}$ .<sup>1</sup> With the SSD, the interaction and the decay vertices of short lived particles will be detected using the change in energy loss in the individual detectors due to change in charged particle multiplicity. In diffractive processes, the interaction vertex can often also be identified.

by a heavily ionizing nuclear recoil while the track multiplicity is relatively small.

The detectors, manufactured and assembled in a telescope with very small spacing, show an increase in the capacitance. Thus to reduce this problem, the sensitive area of each individual detector is partitioned and each partition is connected to a low noise analog pulse processor. The processor consists of a fast, cold resistance head amplifier and a main shaping amplifier. The pile up effect is kept to an acceptable level by shortening the pulse shaping time  $< 100$  ns base width. Thus a single partition can accomodate a counting rate of  $\sim 2 \times 10^6$ .

The SSD spatial resolution depends on the detector spacing and also on the thickness. The choice of the thickness,  $100 - 300 \mu\text{m}$ , is a compromise among resolution, Landau fluctuations, and stochastic noise.

For the charm experiment, the SSD will consist of a set of 40 silicon detectors,  $200-300\mu\text{m}$  thick, whose individual areas are sectioned into 5 parts connected to 200 hybridized analog pulse processors. The cost of this instrumentation is about \$ 200,000 and will be provided by the Milan group.

### 3. Beauty Search

To search for open beauty states at the Tevatron, we will use a "charm trigger" which has been tested at CERN<sup>2</sup> in both a photon

and pion beam (35 GeV/c) and will again be tested there shortly at energies up to 350 GeV.

A target in which beauty particles can be produced will be immediately followed by two detectors, A and B, which are separated by an interval. The interval distance and target distance are chosen so that the greatest number of charmed particles produced in the target will decay in the interval. We will trigger on difference in multiplicity between A and B. The most harmful trigger backgrounds are due to secondary interactions and  $\gamma$  conversions in detectors which can be rejected if A and B are SSD telescopes. From them, a trigger signal is obtained by introducing a majority in  $(N_B - N_A)$  where  $N_A/N_B$  are the real time sum of the pulses from all detectors of the telescopes. Each individual detector is also read out separately to allow off-line analysis of the signal structure as well as further suppress these backgrounds.

The summing of the  $n$  pulses from  $n$  individual SSD detectors increases by a factor  $n^{1/2}$  the stochastic noise of the head amplifiers, while the Landau fluctuations remain unchanged. However, if in summing the 2 or 3 biggest pulses are rejected, the Landau fluctuations are reduced and the pulse distribution shape becomes gaussian-like.

A two-SSD system, A consisting of 5-100  $\mu\text{m}$  individual detectors and B of 10-200  $\mu\text{m}$ , was tested at CERN. The trigger yield of charm events was improved from  $1/(3 \times 10^5)$  to  $1/300$ . With this

encouraging result, several efforts to increase the actual trigger efficiency are underway: decreasing detector capacitance to reduce stochastic noise and redesigning of the processing electronics.

For beam energies of the order of some hundred GeV, nuclear emulsion is the target of choice to measure beauty lifetimes. At the Tevatron, however, the number of possible targets increases and the specific choice will depend on the actual value of the beauty lifetime. If the lifetime is  $> 5 \times 10^{-14}$  s, a SSD target may be equal to the task, especially considering the large beauty/charm mass difference. Thus in the target SSD, beauty is both produced and decays. In A and B, the charmed particle decays are detected (see Fig. 1).

Assuming 50 nb/nucleon  $b\bar{b}$  production cross section and a charm/beauty ratio  $\sim 10^3$ , one  $b\bar{b}$  pair will be produced in every  $6 \times 10^6$  interactions. Triggering on charm, we should obtain out of 6000 triggers, 1000 charm events and 1 beauty event. If the beauty lifetime/beam energy is big enough to use a SSD target, it may be possible to trigger on the beauty decay signal, where the charge multiplicity is  $\sim 14$ .

A spectrometer opening angle of  $\pm 18^\circ$  ensures that more than 80% of the beauty events will be accepted independent of both production and decay mechanisms. This hodoscope and the associated electronics will be provided by the Milan group at a cost of \$ 200,000.

#### 4. The Downstream Spectrometer

Before Tevatron experiments begin in M6W on the Fermilab Multiparticle Spectrometer, E580/623 and E557 will have completed the full compliment of MWPCs and replaced spark chambers with drift chambers. For this experiment we propose to arrange the FMPS as shown in Fig. 2. Moving downstream from the target will be; (A) a 1 mm wire spacing x- and y-pair each with half-wire offset and a u/v-pair; (B) a 2 mm x-, y- and u/v-pair; (C) a 2 mm x- and y-pair in the magnet region; (C<sub>A</sub>) a 44-cell atmospheric Cherenkov counter; (D) a 2 mm x-, y- and u/v-pair; (C<sub>B</sub>) a 30 cell atmospheric Cherenkov counter; (E) two 19 mm cell spacing drift chamber modules each containing an x-pair with a half-cell offset and u/v-pair at  $\pm 16.7^\circ$ ; (F) a 2 mm x/y- and u/v-pair in the beam region; a coarse spatial resolution calorimeter with  $(\sigma/E)_{EM} = .2/E^{1/2}$  GeV (16 r.l. Pb) and  $(\sigma/E)_{HAD} = .7/E^{1/2}$  GeV (7.5 a.l. Fe). The charged track momentum resolution traversing the drift chambers, ignoring multiple scattering, will be  $\pm 4.7 \times 10^{-4} p^2 (\text{GeV}/c)^{-1}$  before spline fitting and  $\pm 2.5 \times 10^{-4} p^2 (\text{GeV}/c)^{-1}$  after. The Cherenkov counters allow  $\pi/K$  separation for momentum between 5.7 - 43.4 GeV/c and K/p separation between 20.5 - 82.4 GeV/c. The production angular acceptance of the device is  $\pm 170$  mrad in the bend plane and  $\pm 93$  mrad out of this plane. The angular resolution in each plane will be  $\pm .25$  mrad.

We discuss here some special improvements we intend to introduce:

#### 4.1. High Resolution Target Chambers

The lack of resolution in the transverse direction produces ambiguous track association between the spectrometer and a specific target decay vertex. Multi-electrode board-backed silicon strip detectors with x,y orientations placed directly up and down stream of the target operated as MWPCs will be used to solve this problem. Prototypes of this type of detector plane have been successfully tested with strip and gap widths of 50  $\mu\text{m}$ .<sup>3</sup> We intend to decrease the grid separation to 25  $\mu\text{m}$ . The microstrip chambers and the associated electronics will be developed by the Milan group at a cost of  $\sim$  \$100,000.

#### 4.2. Electromagnetic Detectors

To study events containing neutral pions and single photons, we need a position sensitive photon detector able to provide  $\gamma/\pi^0$  separation which will be located immediately in front of the calorimeter. Two  $\gamma$ -rays from a 100 GeV  $\pi^0$ , about 10 m away from the target, will be on the order of several millimeters apart from one another depending on the relative energy splitting.

The determination of the center of gravity of the lateral sampling in the early stage of the shower development is then essential to provide the  $\gamma/\pi^0$  separation. This technique has been tested at CERN<sup>4</sup> in different types of calorimeters and

appears to be adequate to our needs. Thus we propose to either add 3 layers of finely grained ( $\sim 5$  mm) plastic scintillators sandwiched with 3 lead sheets 3 - 5 mm thick, or alternately to use in the MWPCs in proportional mode with associated electronics currently under development for  $\nu - e$  scattering experiment. An adequate measurement of the photon energy could be achieved by combining energy information from this finely grained device with the existing Front Hadron and Back Hadron calorimeters.

This shower detector should cost between \$ 50,000 - 200,000 depending on FMPS overall needs, and could be fabricated by Virginia Tech.

#### 4.3. Muon Detector

A low spatial resolution area detector placed after the calorimeter and about 2.5 m of iron shielding will have an area matched to the spectrometer aperture and will be used as a  $> 4$  GeV muon event trigger/tag. The state of the art now permits inexpensive construction of such a device of limited streamer resistive tubes. We propose to fabricate an area detector based on one of these principles at Virginia Tech at a cost of  $\sim$  \$15,000.



References and Footnotes

† Because of space-time limits, this letter has not had the benefit of review by our collaborators in E580/623. As we make clear the details of this experiment, we will invite them to join us. Positive interest will reflect in the addition of names and institutions to the title page.

† Istituto di Fisica and Sezione INFN, Bologna.

1. E. Albin, M. Artuso, G. Bellini, P. d'Angelo, P.F. Manfredi, D. Marioli, E. Meroni, L. Moroni, C. Palazzi-Cerrina, F. Ragusa, P.G. Rancoita, S. Sala, Paper 795 presented at the "XX International Conf. on High Energy Physics", Madison 1980.
2. CERN, Genoa, Milan, Moscow Collaboration, Test Experiment on Beauty; CERN/SPSC/80-02-SPSC/, (1980), 137.
3. E.H.M. Heijne, L. Hubbeling, B.D. Hyams, P. Jarron, P. Lazeyras, F. Piuz, J.C. Vermeulen, A. Wylie, CERN/EF/BEAM 80-6, July 1980.
4. D. Bollini, P.L. Frabetti, G. Heiman, G. Laurenti, L. Monari, F.L. Navarra, Nucl. Instr. and Meth., 171 (1980), 237.

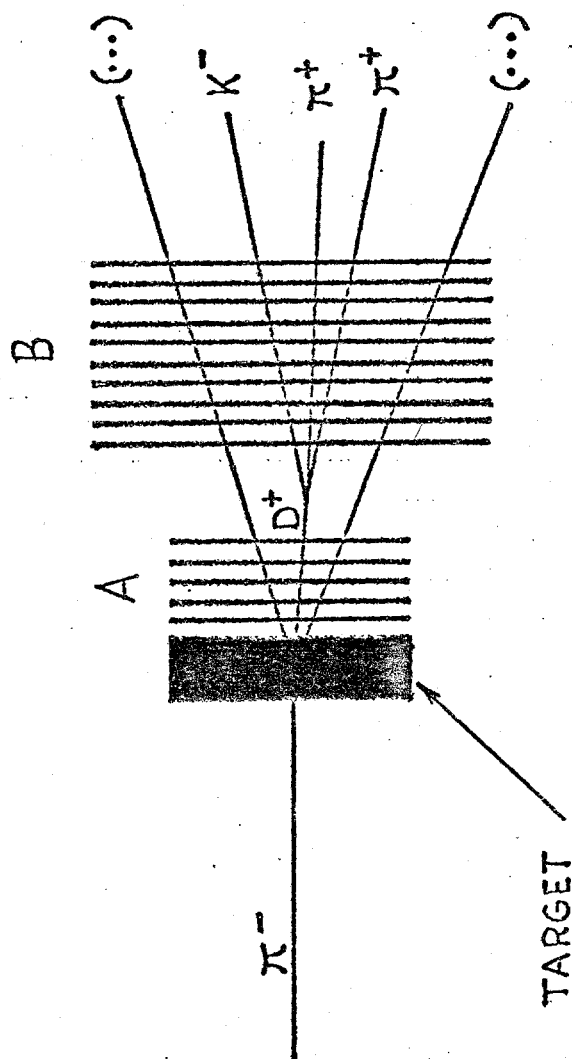


Fig. 1. Sketch of the silicon arrangement for a trigger on charm.

## FMPS LAYOUT FOR CHARM/BEAUTY EXPERIMENT

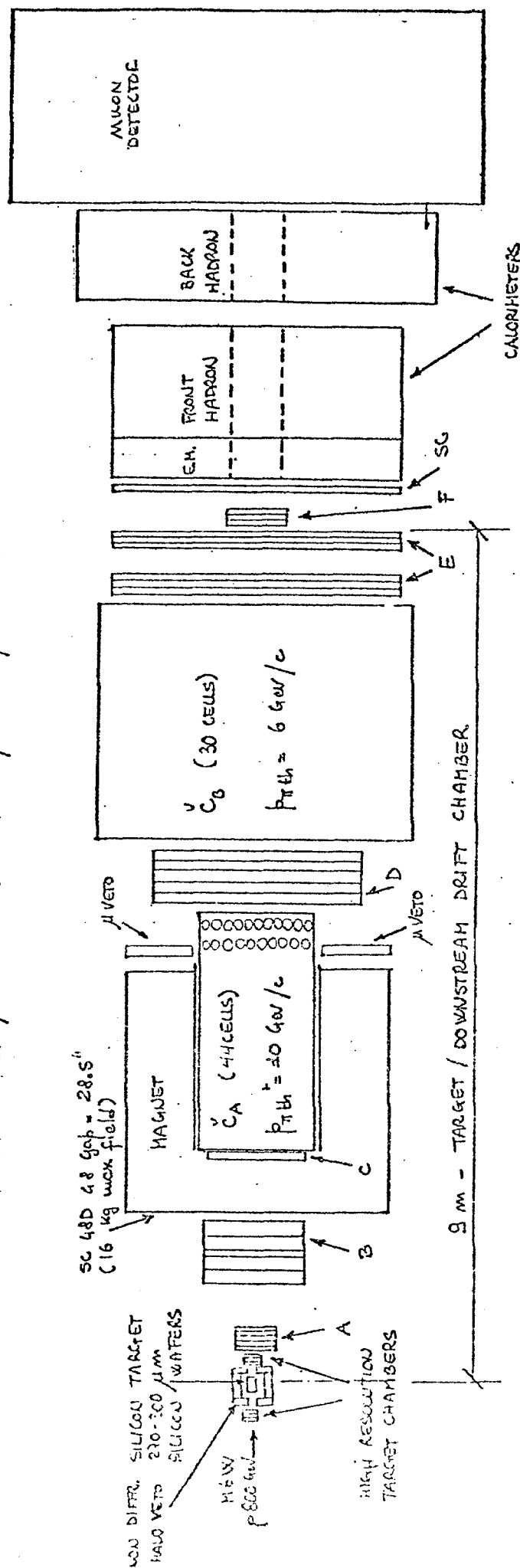


Fig. 2. FMPS layout: plan view: scale 50:1

FERMILAB PROPOSAL 696

Spokesperson:  
W. Peter Trower  
Virginia Tech  
703-961-6230

Arizona/Fermilab/Krawkow/  
Notre Dame/Pavia/Tufts/  
Virginia Tech

Hadroproduced Charm Particles and Their Decay:  
A Proton-Proton FMPS Experiment at the Tevatron

E.W. Jenkins and A.E. Pifer  
University of Arizona, Tucson, Arizona 85721

H.C. Fenker  
Fermilab, Batavia, Illinois 60510

Z. Buja, E. Gladysz, S. Mikocki, M. Szarska and L. Zawiejski  
Institute of Nuclear Physics, Krakow POLAND

C-C. Chang, T.C. Davis, K.J. Johnson and J.A. Poirier  
University of Notre Dame, Notre Dame, Indiana 46556

P.E. Argan, F. Fossati, P. Pedroni and T. Pinelli  
Istituto di Fisica Nucleare and Sezione INFN, Pavia ITALY

W.A. Mann, A. Napier and J. Schneps  
Tufts University, Medford, Massachusetts 02155

J.R. Ficenec and W.P. Trower  
Virginia Polytechnic Institute and State University,  
Blacksburg, Virginia 24061

(February 1, 1983)

## Table of Contents

|   | <u>Page</u> |
|---|-------------|
| Summary .....   | 3           |
| I. Introduction .....   | 4           |
| II. Physics Goals .....   | 5           |
| A. Open Charm .....   | 5           |
| B. Open Beauty .....  | 7           |
| C. $\phi$ Final States .....  | 7           |
| III. Topologies and Rates .....   | 8           |
| A. $F(cs)$ .....  | 8           |
| B. $B(cd)$ .....  | 10          |
| IV. Apparatus .....   | 10          |
| V. Triggers .....   | 13          |
| VII. Analysis .....   | 15          |
| References .....  | 16          |
| Tables  |             |
| I. Cross Sections for Hadronic Charm Production .....                           | 17          |
| II. Chamber Characteristics .....   | 18          |
| III. Gas Cherenkov Thresholds .....   | 19          |
| VI. Spectrometer Aperatures .....   | 19          |
| V. Trigger Types .....  | 20          |
| Figures   |             |
| 1. Inclusive F hadroproduction cross section at $\theta_{cm} = 45^\circ$ . .... | 21          |
| 2. Experimental Layout. ....  | 22          |
| 3. Target Box. ....   | 23          |
| 4. $K_S^0$ Decay Probability vs. $X_F$ . ....                                   | 24          |
| 5. $K_S^0$ Acceptance vs. $(X_F, P_T)$ .....                                    | 25          |

### SUMMARY

We propose to measure open charm production in proton-nucleon collisions at the highest Tevatron energies using the Fermilab Multiparticle Spectrometer (FMPS) in the M6W beam line. Specifically, we will focus on the most uncertain charmed meson, the  $F(cs)$ . Instrumentally and philosophically this experiment is an enhanced continuation of our completed and partially analyzed experiments E580 ( $\pi^- p \rightarrow V^0 V^0 X$  at 200 GeV) and E623 ( $p p \rightarrow \phi \phi X$  at 400 GeV). With our trigger we should be able to access other open charmed states, search for gluonium, and look at the high transverse momentum ( $P_T$ ) events for evidence of open beauty production.

This experiment would use the existing FMPS including the modifications currently being made for E557. We would add a second bending magnet, silicon strip chambers immediately before and after the target, high pressure PWCs near the target, and two Cherenkov counters downstream of the existing bending magnet. These modifications with the existing apparatus would allow a precise determination of the interaction vertex to investigate short lifetime decays, measurement of charge particle production angles and momentum, and identification of several charged kaons over a wide range of momentum.

We request 1600 hours of M6 beam at  $3 \times 10^7$  protons/(10-second spill) with a repetition of 1 spill/minute - half of the FY84/5 M6 running period.

## I. INTRODUCTION

Our considerable knowledge of charmed particles has come mainly through their observation in  $e^+e^-$ , photoproduction, and neutrino reactions. The detection of hadroproduced charmed particles and the measurement of their production cross section has been very difficult. Although we now have an excellent understanding of charmonia, the  $J/\psi$  states, we are less well informed about the  $D$  and  $\Lambda_c$  open charm states, and are woefully ignorant of the  $F$ . It is the  $F$  which also holds extrinsic interest as a source of  $\nu_\tau$  from proton beam dumps.<sup>1</sup>

The detection of open beauty has been even more difficult than open charm and none have been seen through reconstruction of their decay products.

Finally, the theoretical speculation that gluons may agglomerate into objects called gluonium has recently gained some credence with the report of two such states which were untangled in a partial wave analysis of a recent Brookhaven experiment. However, a high statistics experiment which shows clear resonant structure whose quantum numbers do not fit in the  $SU(3)_C$  ordering scheme would constitute the strongest experimental evidence for the existence of the gluon.

Our fast logic will identify several charged kaons and  $V^0(K_S^0, \Lambda, \bar{\Lambda})$  candidates, and kinematically determine one or more  $\phi(K^+K^-)$  in each interaction. With this information we will record events based on a hierachial decision whose logic will rely on the probability of a combination containing an  $F$ . In this sample, which could contain about 50 million events, there will be ample data to investigate the production of other open charm states, possibly open beauty, and gluonium. Further, the prospects for determining lifetimes from the identified and reconstructed charm events are promising.

## II. Physics Goals

Our physics goals in this experiment are three. First, we wish to contribute experimental information on the hadroproduction and decay of open charm states. Here we concentrate on the detection of the  $F(cs)$  because its properties are still largely unknown. By constructing an  $F$  trigger we will also capture analyzable samples of the other better understood open charm states. Second, we will attempt to see open beauty by two strategies. If a sufficiently large number of identified charm particle events can be obtained, then a parent beauty particle can be sought as an enhancement in the mass distributions, especially in the double charm particle events. Also requiring at least one large  $P_T K^\pm$  in the trigger should increase the probability that open beauty may be present. Third, we would like to extend our study of  $\phi$  production to higher energies and multiple  $\phi$ s in order to investigate, among other things, the possibility of gluonium. As our proposed run is two years hence, we will be vigilant for new physics possibilities to include in our program.

### A. Open Charm

It is significant that charmed particles were simultaneously discovered by electroproduction with colliding beams and hadroproduction in a fixed target experiment. This initial synchrony of source and technique has continued as the experimental facts of this new particle family have been revealed. Our current knowledge of hadroproduced charmed particles is summarized in Table I, while the Review of Particle Properties<sup>2</sup> summarizes the decay branching ratios.

Most of the best information on the decay modes and branching ratios of the  $D$  mesons come from  $e^+e^-$  colliding beam experiments which produce low background event samples. Our knowledge of the  $F^\pm$ ,  $\Lambda_C^+$ , and  $\Sigma_C^+$  existence, production, decay, and lifetimes have come mostly from emulsion hybrid systems exposed to



photon/neutrino beams at fixed target proton accelerators. Recent hadroproduction results at Fermilab and CERN now show evidence of charmed particle production although the backgrounds are large.

Our knowledge of the charmed particle lifetimes, typically tenths of picoseconds, is currently sketchy due to low statistics. The  $F_c^\pm$ ,  $\Lambda_c^+$ , and  $\Sigma_c^+$  lifetimes are less well known than those of the Ds, furthermore the prospects for substantially improving lifetimes other than the D are not encouraging. F meson decays are seen in  $\eta\pi$ ,  $\eta^3\pi$ ,  $\eta^5\pi$ ,  $\phi\rho$ ,  $(3\pi)^\pm\pi^0$ ,  $K^+K^-\pi^\pm$ ,  $K^+K^0(2\pi)^0$  and  $K^+K^-\pi^\pm\pi^0$ . Cabibbo favored decays may not dominate here.

Data which would specify the production process for open charm is sparse and often conflicting while the theoretical understanding is confused and therefore can not provide a reliable guide for an experiment. For example, theoretical estimates for central charm production lead to D cross sections of about 1  $\mu\text{b}$  at 350 GeV/c while experimental results give 10-40  $\mu\text{b}$ . Production cross sections at the ISR now appear to be even larger, 100-1000  $\mu\text{b}$ . Theoretical estimates of peripheral charm production are even smaller; for example, pions will create  $D^-\Lambda^+$  at 0.5 nb and D's inclusively at 60 nb. Evidence for diffractive production of charged D pairs at Fermilab with 217 GeV/c pions yields a cross section of  $(6-10)\pm 4$   $\mu\text{b}$ . Photoproduction experiments appear to yield conflicting results. Results from CERN suggest the dominant mechanism is  $D\Lambda_c X$  while the Fermilab results at higher energies imply DDX dominance. Photoproduction of the F meson at CERN yields for example,  $\sigma_B(\eta^3\pi) = 30\pm 18$  nb.

Diffractive production of FF pairs in coherent scattering would require an  $s\bar{s}$  and  $c\bar{c}$  pair to be extracted from the sea. The experimental information about  $F_c^\pm$  and  $\Lambda_c^+$  is sketchy as is the theoretical understanding of these results. Clearly there is much to be learned here.

A leading order perturbative QCD calculation of  $p p \rightarrow F^+ X$  has been made and

evaluated for several choices of distribution/fragmentation functions.<sup>3</sup> Figure 1 shows the cross sections at fixed  $F$  center-of-mass scattering angle as a function of  $P_T$  of the  $F$  for proton momentum of 0.4 (—) and 1 (---) TeV/c. The contributions from the individual graphs are indicated. Note that diffractive production, gluon-charm quark elastic scattering, provides that majority of the cross section.

### B. Open Beauty

The four well studied members of the  $T$  family have firmly established the existence of the  $b$  quark. Although there is experimental indication of open beauty in the variation of the total cross section and the  $K/\pi$  ratio, no reconstructible individual open beauty particle has been seen. What is known is that hadroproduction is small,  $B(T \rightarrow \mu\mu) \cdot (d\sigma/dy)_{y=0} \sim$  few pb/nucleon at 400 GeV/c.<sup>4</sup> Further, the beauty mesons should have masses 5-7 GeV/c<sup>2</sup> and lifetimes are predicted to be  $\sim 10^{-14}$  seconds.<sup>1</sup> A highly probable decay mode would produce two charm particles (e.g.,  $B^0(b\bar{d}) \rightarrow D^+F^-$ ) each of which could have a substantial  $P_T$  as the energy available in the decay is significant. This in turn would yield large  $P_T$  kaons.

### C. $\phi$ Final States

The production dynamics of the single  $\phi$  system can be used to investigate the question of how hidden strangeness is compensated for in  $\phi$ . If it is, does the compensation occur locally or globally?

The  $\phi\pi^\pm$  system is Okubo-Zweig-Iizuki (OZI) forbidden for the decay of any  $q\bar{q}$  meson. Its existence would either violate the OZI rule or indicate a weak decay (e.g.,  $F^\pm \rightarrow \phi\pi^\pm$ ) or a multiquark (e.g.,  $q\bar{q}q\bar{q}$ ) allowed decay.

In the  $\phi\phi$  system the  $q\bar{q}$  states must be even under charge conjugation and so they will not decay into  $e^+e^-$  or  $\mu^+\mu^-$ , both favorite for most charm particles.

The  $\eta_c$  at  $3 \text{ GeV}/c^2$  and the  $\eta_b$  at  $\sim 10 \text{ GeV}/c^2$  should both be present at the level of some tens of nanobarns at 1 TeV incident proton energy.

Great theoretical interest has been generated in the possibility of pure gluon bound states. Recently, some experimental indications that such states might exist were obtained using a sample of 1203 events obtained in the reaction  $\pi^- p \rightarrow \phi\phi n$  at  $P_{\pi^-} = 22(\text{GeV}/c)$ .<sup>5</sup>

### III. TOPOLOGIES and RATES

The event topologies on which we will trigger will be combinations of four separate inputs; probable  $V^0$  (as determined by changes of 2,4,6 in the number of hits on PWC chamber arrays upstream and downstream of the decay volume); charged kaons (as determined by the absence of a Cherenkov counter signal from a roughly reconstructed track whose momentum is sufficient for a pion to produce light in that cell);  $\phi$  (as determined from the reconstructed mass from the rough momentum of two unlike charged kaons); and probable charm, C, (as determined by a change of 2,4,6 in the number of hits on two pairs of silicon strip chambers in the target box). So for example, the topology (1  $V^0$ , 1  $K^\pm$ , 0  $\phi$ , 1 C) would contain  $F^\pm \rightarrow K_S^0 K^\pm$  where the F lifetime may be measurable.

#### A. F(sc)

F decay modes and branching ratios are still largely unknown. The decay  $F \rightarrow \pi^\pm \eta$  was reported in  $e^+e^-$  data from DASP<sup>6</sup> but the Crystal Ball at SPEAR<sup>7</sup> was not able to reproduce the large energy dependence of the  $\eta$  production near  $FF^*$  and  $F^*F^*$  thresholds. A solitary neutrino induced event, recorded in emulsion placed in front of the 15-foot bubble chamber,<sup>8</sup> fit  $F^+ \rightarrow \pi^+\pi^+\pi^-\pi^0$  but also had a likely interpretation as  $\pi^+\omega$ . Two neutrino events in emulsion<sup>9</sup> produced  $F^- \rightarrow \pi^-\pi^-\pi^+\pi^0$  and  $F^+ \rightarrow K^+\pi^-\pi^+K^0$  fits while 2 other events were ambiguous with charged D mesons. Five F candidates out of 21 charm events in 95,000 interactions were

found in the NAL8 340 GeV  $\pi^-$  exposure with BIBC,<sup>10</sup>  $2 F^- \rightarrow K^+ K^- \pi^-$ ,  $2 F^- \rightarrow \pi^- \pi^- \pi^+$  and  $1 F^+ \rightarrow \pi^+ \pi^+ \pi^- \pi^-$ . This experiment did not have particle identification or  $\pi^0$  detection. LEBC<sup>11</sup> reports 3 unambiguous F decays in  $\pi^- p$  and  $pp$  interactions at 360 GeV;  $F^\pm \rightarrow K^+ K^- \pi^\pm \pi^0$  and also 3 ambiguous  $F^\pm/\Lambda_c^+$  decays. The 182,000  $pp$  interaction exposure produced 35 charm decays. The NAL photoproduction experiment<sup>12</sup> with photon energies up to 150 GeV report observing  $F^+ \rightarrow \eta \pi^+ \pi^- \pi^+ \pi^0$  and  $F^+ \rightarrow K^- K^+ \pi^+ \pi^0$ , including  $F^+ \rightarrow \phi \pi^+ \pi^0$ , with the kaon channel being favored by at least a factor of 2 with respect to the  $\eta$  channel. The number of observed  $\eta$  events is  $\sim 9$ . There are multiple combinations of final state particles. WA4 reports<sup>13</sup> photoproduction of  $F^\pm \rightarrow \phi \rho^\pm$ ,  $\eta \pi^\pm$ ,  $\eta(3\pi)^\pm$ , and  $\eta'(3\pi)^\pm$ .

We now estimate the F event rates. A 1600 hour run at  $3 \times 10^7$  protons/spill will provide  $3 \times 10^{12}$  protons on target during the 96,000 10-second one-per-minute spills. A 10% target will produce an interaction rate of  $3 \times 10^5$ /second. A modest data logging rate of  $10^3$  events/spill could produce  $10^8$  triggers, in reality more like  $5 \times 10^7$  will be collected. About 10% of these will be good based on our E623 experience with the  $\phi\phi$  and  $K^+ K^- K^+ K^-$  trigger. Using BIBC results assuming a 20% efficiency we should see in excess of  $\sim 500$  F decays in all charged final states. LEBC data assuming a 10% efficiency predicts in excess of 800  $K^+ K^- X$  events. The F cross section can be estimated from the LEBC data by scaling the inclusive D cross sections by the  $K/\pi$  ratio,  $\sim 6$   $\mu\text{b}/\text{nucleon}$ , or by scaling the number of F decays by the experimental sensitivity to get a lower limit,  $\sim 5$ -10  $\mu\text{b}/\text{nucleon}$ . If half the time  $F \rightarrow KKX$  of which 1/4 will be charged, while 16%/44% of the charged/neutral Ds result in  $K^\pm$ , then, if FDK associated production dominates and half the kaons are charged, the fraction of FDK final states that will be observed as  $K^+ K^- K^+ K^-$  is  $\sim (.125) (.15) (5 \mu\text{b}) = 95 \text{ nb}$ . If  $F^+ F^-$  associated production dominates, then the cross section to four charged kaons is expected to be larger.

Backgrounds can be estimated from inclusive K production results and our preliminary E623 data. As the inclusive charged 4K cross section is  $\sim 400$   $\mu\text{b}/\text{nucleon}$ ,  $\sim 2 \times 10^{-4}$  of the  $K^+K^-K^+K^-$  events would contain an F. Hence  $\sim 2 \times 10^{-5}$  of the triggers would contain an F, yielding 1000 F events during our run. Since the number of F events with  $K^+K^-K^+K^-$  produced forward during a spill would be  $\sim 100$ , a trigger more selective than the one used in E623 would enhance our signal to background and increase the F event sample. The short decay charm trigger, C, using the silicon chambers in the target box should increase the signal by a factor of 10 relative to the background.

#### B. B(cd)

Using the diffractive charm production cross sections indicated in the 1980 ISR results, the cross section at the Tevatron may be as much as 500  $\mu\text{b}/\text{nucleon}$ . If we assume a charm/beauty ratio of  $\sim 10^3$  then one b $\bar{b}$  pair should be produced in every  $10^5$  interactions whose decay products would have an estimated charge multiplicity of  $\sim 14$ . Calculating as in the case above, we would have one b $\bar{b}$  event in every spill, to be compared with  $\sim 100$  F events/spill. Hence, without a more selective trigger we would collect only 10 beauty events. From E623 experience we estimate that a  $P_T$  cut would give a factor of two enhancement, while the short decay trigger will give a factor of ten to give 200 beauty events.

#### IV. APPARATUS

Figure 2 shows an plan view of the FMPS in the plane of the undeflected beam as configured for our experiment. Not shown are two upstream beam measuring stations, BM1 and BM2. Chamber position and characteristics are given in Table II. Timing and beam definition will be determined by scintillators BS1 • BS2 • BS3 located directly upstream of the third beam measuring station, BM3. A thin

(10% interaction probability) heavy metal target, sectioned into three parts, will be interspersed in 3 silicon strip chamber stations (S1-3). This entire unit is the target box. These chambers will provide multiplicity and position information to a fast trigger processor to enhance the signal to background. Figure 3 shows the arrangement of silicon chambers and target elements within the target box. With S1-3 the interaction vertex will be determined to within a few microns and together with the high pressure PWC system, H, they will allow the reconstruction of outgoing tracks to aid in short lifetime particle identification. The PWC stations H/A/B/C/D, in addition to providing information for charged particle track reconstruction, will provide fast multiplicity information upstream and downstream of the decay regions which will be used in some triggers to indicate the presence of neutral  $V^0$  as was done in E580. The  $V^0$  decay regions (3.4m long) contain helium bags and extend from stations H to A, and from stations A to B, the same region occupied by the first bending magnet (M1). M1 will be a modified BM109 with an 0.36m vertical gap that provides 0.676 GeV/c transverse momentum kick, matching that of M2, the present superconducting spectrometer magnet. Atmospheric threshold Cherenkov counter,  $C_B$ , will provide charged particle mass identification over the entire spectrometer aperture. Helium, neon, and nitrogen gas mixtures will be used to adjust these thresholds. Table III gives thresholds for each of these gases and a typical mix. PWC stations B/D with drift station DR and Cherenkov  $C_B$  will provide information to a fast trigger processor similar to that used in E623<sup>14</sup> for identification of multiple charged kaons,  $\phi$  and  $\phi\phi$ . PWC station E will be placed downstream of the drift station and will provide charged particle position information over a slightly smaller aperture than the drift station. Two additional smaller aperture PWC stations, F and G, and Cherenkov  $C_C$  will be used to resolve fast forward charged tracks, and to identify fast kaons and

protons in the forward region.

Much of the hardware just described is available or will be available at the FMPS by 1984. The items that we will fabricate are: S1-3, H,  $C_B$  and  $C_C$ . Since both Cherenkov counters have potential use for other approved experiments in M6 which are scheduled after we would run, every effort will be made to build and design these devices to easily facilitate adding upstream attachments in order to increase radiator length.  $C_C$  will use the mirrors and phototubes formerly used in  $C_A$  of E623 and the redesigned  $C_B$  will use as much from the previous  $C_B$  counter as possible. It is expected that Fermilab would provide the beam measuring stations BML-3 and the modified BML09 magnet ML.

Photon detection, both position and energy, and the reconstruction to  $\pi^0$  and  $\eta$  would significantly enhance our detection of the F through decay modes which contain these particles. We continue to investigate the most effective ways to compliment the calorimeter and forward lead glass array that will be available at the FMPS. For example, by restacking the E557 lead glass we could cover the forward downstream aperture. All cell sizes in the central region are  $3.8 \times 3.8$  cm<sup>2</sup> and in the outer region are  $10 \times 10$  cm<sup>2</sup>. The wide angle photons would be measured by a  $\gamma$ -chamber placed immediately upstream of the calorimeter. This  $\gamma$ -chamber is 4rℓ fronted, sampling, delay line PWC of the type recently developed by Nunamaker for an axion search at SLAC.

The spectrometer aperture, summarized in Table IV, is essentially  $\pm 72$  mr horizontally and  $\pm 42$  mr vertically for high momentum particles. The forward small angle extension of the spectrometer subtends  $\pm 20$  mr horizontally and  $\pm 13$  mr vertically. The resulting angular resolution for produced charged tracks is  $\pm 0.13$  mr, and for the tracks materializing in the decay volume is  $\pm 0.2$  mr. The charged particle fractional momentum resolution after fitting, ignoring multiple scattering, is estimated to be  $0.7 \times 10^{-4}$  P(GeV/c) for the full spectrometer and

$3 \times 10^{-4} P(\text{GeV}/c)$  for the upstream half (target to C station) or the downstream half (B station to E station). Slight improvements can be expected for the very fast forward particles that traverse the small angle extension. The resulting mass resolution in  $\text{MeV}/c^2$  is  $\Delta m(K_S^0 \rightarrow \pi^+\pi^-) \sim P_{K_S^0}(\text{GeV}/c)/4$  and  $\Delta m(\phi \rightarrow K^+K^-) \sim P_{K^\pm}(\text{GeV}/c)/10$  for symmetric decays. Fractional photon energy resolution in the E557 calorimeter is  $0.013 + 0.2/\sqrt{E}(\text{GeV})$ , and in the lead glass is  $0.013 + 0.106/\sqrt{E}(\text{GeV})$  for the central region and  $0.013 + 0.064/\sqrt{E}(\text{GeV})$  for the outer region. Position resolution in the  $\gamma$ -chamber is 1 mm and in the lead glass is  $2/3$  mm in the central/outer regions. The resulting  $\pi^0 \rightarrow \gamma\gamma$  mass resolution at 3 GeV is 9 MeV/6 MeV for the central/outer regions of the lead glass and 17 MeV for the  $\gamma$ -chamber-calorimeter assuming a symmetric decay. At 100 GeV, the mass resolution is  $\sim 7$  MeV for all detectors. The E557 calorimeter will only allow unambiguous  $\pi^0$ ,  $\eta \rightarrow \gamma\gamma$  particle reconstruction when a single photon enters a cell, whose sizes range from  $10 \times 20 \text{ cm}^2$  at the small angles to  $30 \times 30 \text{ cm}^2$  at the largest angles. Multiple photons in a cell and their association with parent particles will be handled on a probabilistic basis.

Figure 4 gives the  $K_S^0$  fraction materializing in the decay volume for  $P_T = 0$  as a function of  $X_F$ . All daughter pions will be measured in the spectrometer when  $X_F > 0$ . Figure 4 shows the  $K^\pm$  center of mass acceptance as contours in the  $X_F$ - $P_T$  plane.

## V. TRIGGERS

To enhance the fraction of charm events in our data sample and to study beauty, we plan to supplement the E580/623 fast triggers with a fast trigger incorporating the silicon detectors. The 10% target is divided into three sections of 3.2 mm W. Each target section (i) is followed by one pair of XY strip chambers 12 mm from the target and a second pair 36 mm from the target.



For central F production, we will look for a change in multiplicity between the first and second pair, presumably from a D decay, to enhance the quality of the F signal. For example, a D meson produced at  $X = .2$ , has a mean path length of 19 mm assuming a  $6 \times 10^{-13}$  sec lifetime. The mean path of the associated F at this same X would be 6 mm, and it would most probably decay before the first pair of chambers. In addition to multiplicity changes, the inclusive cone of charged particle trajectories defined by both pairs of chambers could be used to signal the presence of a vertex downstream of the target. These reconstruction and multiplicity tests will be accomplished in a fast processor parallel to the charged kaon defining processor (E623). Diffractively produced F's with their significantly higher momentum would typically decay between the two pairs of chambers to provide a direct trigger signal. The chamber sections downstream of the interaction section (i+1, i+2) will be used to tighten the trigger requirements and accurately define the particle trajectories. We estimate that the sample of F and B candidates could be increased by a factor of 10 by this technique. Finally, we are investigating fast post trigger processors that would allow us to accumulate 5,000-10,000 triggers per spill and then reduce the number of events put onto tape by a factor of 5 to 10 thereby increasing our F and B candidates by a factor of 5-10.

The neutral vee and charged kaon trigger requirements and the potential charm content resulting from these is summarized in Table V for an idealized trigger. Our experience with E580/623 indicates that a trigger requiring a charge multiplicity change of 4 in a decay volume yields a  $1 V^0$  event 50% of the time and a  $2 V^0$  event 6% of the time, and a trigger requiring 2  $\phi$ 's yields  $4K^\pm$  10% of the time, a single  $\phi$  1% of the time and  $\phi\phi$  0.1% of the time. Hence the actual operating triggers will be set more rigidly based on previous experience to accommodate the trigger inefficiencies. We will saturate our trigger rate by

selectively reducing or expanding a given set of requirements, for example, by accepting every Nth trigger of a given type or by reducing the  $P_T$  requirement somewhat.

## VII. ANALYSIS

If the  $5 \times 10^7$  triggers were processed through the E580/E623 software, at  $\sim 1$  CPU second/event for and track finding and a like amount for kinematics, more than 2 CPU years would be required to reduce the data. Thus, we propose to modernize our present analysis procedure; convert existing code from Fortran to assembly language, and modify some algorithms (e.g., we estimate that a fast decision to keep/discard an event could be made in  $\sim 1/10$  second based only target box information.). Such changes could decrease rough data reduction time to  $1/10$  CPU year. A like amount of CPU time would be required to complete the track finding and kinematics on the remaining events. If the number of F candidates is then reduced to  $\sim 10^4$  we will need only  $10^4$  additional CPU seconds to complete the processing. The total experiment computing requirement is  $\sim 3-4$  CPU months.

We intend to examine the possibility of using microprocessors for additional preprocessing of online data before writing anything on tape. Perhaps the long interspill time, 50 seconds, can be utilized effectively by the online computer as well. Replacing/augmenting the existing PDP11/45 by a faster computer would clearly help.

REFERENCES

1. V. Barger, J.P. Leville, D.M. Stevenson and R.J.N. Phillips, Phys. Rev. Lett. 45, 83 (1980).
2. M. Roos et al., Phys. Lett. B111 , 1 (1982).
3. N.S. Craigie, F. Hussain, K. Khan, S Mahmood and W.P. Trower, VPI-EEP-83-2.
4. K. Ueno et al., Phys. Rev. Lett. 42 , 486 (1979).
5. A. Etkin et al., Phys. Rev. Lett. 49 , 1620 (1982).
6. Brandelik et al., Phys. Lett. B70 , 132 (1977); and Brandelik et al., Phys. Lett. B80 , 412 (1979).
7. Partridge et al., Phys. Rev. Lett. 47 , 760 (1981).
8. Ammar et al., FERMILAB-80/39-EXP (1980).
9. Ushida et al., Phys. Rev. Lett. 45 , 1053 (1980).
10. Results of the charm search with BIBC, NA18 collaboration, Paris, 1982.
11. Aguilar-Benitez et al., CERN/EP 82-188 (1982); CERN/EP 82-203 (1982); and CERN/EP 82-204 (1982).
12. Amendolia et al., CERN/EP 82-200 (1982).
13. Aston et al., Nucl. Phys. B189 , 205 (1981); and Aston et al., Phys. Lett. B100 , 91 (1981).
14. H.C. Fenker, D.R. Green, S. Hansen and T.F. Davenport, FERMILAB-82/62-EXP.

TABLE I. Cross Sections for Hadronic Charm Production

| Expt Type* | Group      | Channel   | Energy /Beam                                     | $\sigma$  |
|------------|------------|---|--|---|
|            | BIBC       | C   | 340 $\pi^- p$                                    | $30 \pm 10 \mu\text{b}/N$ if $\sigma \propto A$<br>$80 \pm 20 \mu\text{b}/N$ if $\sigma \propto A^{2/3}$  |
|            | LEBC-EMS   | $D^\pm$ incl.<br>$D^0$ incl.  | 360 $\pi^- p$                                    | $8 \pm 4 \mu\text{b}$ in $X_F > 0$<br>$\sqrt{8 \pm 4 \mu\text{b}}$ in $X_F > 0$   |
| bh         | CYCLOPS    | pD $\bar{D}X$   | 225 $\pi^- p$                                    | $\sim 40 \mu\text{b}^1$ for $D \rightarrow K\pi\pi, K\pi; \bar{D} \rightarrow \mu X$  |
| bh         | ABCCMR     | $D^{0*} \bar{D}^0, D^0 \bar{D}^0 X$<br>$\Lambda_c^- \bar{D}^- X$  | 200 $\pi^- \text{Be}$<br>150 $\bar{p} \text{Be}$ | $5 \pm 2 \mu\text{b}^1$ for $D \rightarrow K\pi\pi, K\pi; \bar{D} \rightarrow eX$<br>$75 \pm 150 \mu\text{b}$ for $\Lambda_c^- \rightarrow K^- p \pi^+$ ; $D^- \rightarrow eX$  |
| bh         | FPS        | $D^{\pm*} X$  | 200 $\pi^- \text{Be}$                            | $4 \pm 1 \mu\text{b}^1$ for $D^{\pm*} \rightarrow D^0 \pi^\pm \rightarrow K\pi\pi^\pm$  |
| hrhbc      | LEBC       | $D^\pm X$   | 360 $\pi^- p$                                    | $11 \pm 5 \mu\text{b}^1$  |
| et-bh      | CCMK (ISR) | $D^+ \rightarrow K^+ \pi^+$   | 31x31 p p  | 0.16, 0.32, 0.80 mb <sup>1</sup>  |
|            | -          | $D^0 CX$<br>$D^0 \bar{D}^0 X$   | 55 $\pi^- \text{Be}$<br>55 $\pi^- \text{Be}$     | $< 10 \mu\text{b}/N^2, < 20 \mu\text{b}/N^3$<br>$< 2 \mu\text{b}/N^2, < 9 \mu\text{b}/N^3$  |
|            | NALL       | $D^0, D^0 X$  | 175 $\pi^- N$                                    | $19 \pm 6 \mu\text{b}$  |
| et-bh      | CBI (ISR)  | $D^0 \rightarrow K^- \pi^+$   | 31x31 p p  | $> 5 \text{mb}$   |
|            | NALL       | $\Lambda_c^- X$   | 150 p Be   | $75 \pm 50 \mu\text{b}/N$   |
| et-bh      | LSM        | $p^+ X$<br>$\Lambda_c^- \rightarrow K^- p \pi^+$  | 31x31 p p  | $\Delta\sigma = B^{-1} (3.1 \pm 1.6 \mu\text{b}^4), \frac{\Delta\sigma}{\Delta X} = 240 \pm 120 \mu\text{b}$<br>$1.2 \pm 0.5 \text{mb}^1$   |
|            | UCLA       | $\Lambda_c^- X$<br>$\Lambda_c^- \rightarrow \Lambda^0 \pi^+ \pi^+ \pi^-$<br>$\Lambda_c^- \rightarrow K^- p \pi^+$   | 31x31 p p  | $\frac{\Delta\sigma}{\Delta X} = 700 \pm 90 \mu\text{b}$ for $.75 < 1X_F < .9$<br>$\sigma \cdot B = 5.6 \pm 2.0 \mu\text{b}$<br>$\sigma \cdot B = 4.6 \pm 0.6 \mu\text{b}$  |
|            | SFM        | $\Lambda_c^- X$<br>$\Lambda_c^- \rightarrow K^- p \pi^+$<br>$\Lambda_c^- \rightarrow \Lambda \pi^+ \pi^+ \pi^-$<br>$\Lambda_c^- \rightarrow K^- p \pi^+$<br>$\Lambda_c^- \rightarrow \Lambda \pi^+ \pi^+ \pi^-$<br>$\Lambda_c^- \rightarrow K^{*0} p$<br>$\Lambda_c^- \rightarrow K^- \Delta^{++}$<br>$\Lambda_c^- e^- X$ | 31x31 p p  | $270 \rightarrow 560 \mu\text{b}^1$<br>$0.7 \rightarrow 1.8 \mu\text{b}$ in $.3 < X_F < .8$<br>$0.3 \rightarrow 0.7$ in $.8 < X_F < .975$<br>$4.6 \pm 0.6 \mu\text{b}$ in $.75 < X_F < .9$<br>$5.6 \pm 2.0 \mu\text{b}$<br>$3 \rightarrow 6 \mu\text{b}$<br>$3 \rightarrow 6 \mu\text{b}$<br>$184, 750, 1125, 4200 \mu\text{b}^1$ |
| et-bh      | CBF        | $\Lambda_c^- \rightarrow K^- p \pi^+$   | 31x31 p p  | 0.2, 0.8, 1.1, 4.2 mb <sup>1</sup>  |
| et-bh      | ACCDMW     | $\Lambda_c^- \rightarrow \Delta^{++} K^-$<br>$\bar{K}^* p$  | 31x31 p p  | $\sim 2.0 \text{mb}^1$<br>$\sim 1.0 \text{mb}^1$  |
| bh         | LAS        | $\Lambda_c^- \rightarrow \Lambda^0 \pi^+ \pi^+ \pi^-$<br>$K^- \pi^+ p$  | 31x31 p p  | $\sim 1.0 \text{mb}^1$<br>$\sim 1.0 \text{mb}^1$  |

h=bump hunt; hrhbc=high resolution hybrid bc; et-bh=electron triggered bh.  
 Model dependent. <sup>2</sup>Diffraction production. <sup>3</sup>Produced as  $J/\psi$  particle.  
<sup>4</sup> $\Lambda_c^-$  cross section for  $10 < M_X < 28 \text{GeV}$ ,  $.5 < X_F(\Lambda_c^-) < .8$ , and  $B(\Lambda_c^- \rightarrow K^- p \pi^+)$ .

TABLE II. Chamber Characteristics

| Station | Electrode Spacing (mm) | Plane Orientation*  | Type          | Number of Wires                  | Active** Area XxY (m <sup>2</sup> ) | <Z (m)>        | Status                 |
|---------|------------------------|---|---------------|----------------------------------|-------------------------------------|----------------|------------------------|
| BM1,2,3 | 1                      | xx'yy'<br>uv ( $\pm 30^\circ$ )   | PWC           | 3(4x128)<br>3(2x64)              | 0.13x0.13                           | -              | Fermi                  |
| S1,3    | .02                    | x <sub>1</sub> x <sub>2</sub> y <sub>1</sub> y <sub>2</sub><br>uv ( $\pm 45^\circ$ )                                  | Si            | -                                | 0.03x0.03                           | -0.07<br>+0.22 | P696<br>P696           |
| S2      | .02                    | 3(x <sub>1</sub> x <sub>2</sub> y <sub>1</sub> y <sub>2</sub> )   | Si            | -                                | 0.03x0.03                           | -              | P696                   |
| H       | .25                    | xx'yy'<br>uv ( $\pm 45^\circ$ )   | PWC<br>(Pres) | 4x256<br>2x256                   | 0.06x0.06                           | 0.4            | P696                   |
| A       | 1                      | xx'yy'<br>uv ( $\pm 45^\circ$ )   | PWC           | 4x256<br>2x256                   | 0.26x0.26                           | 1.8            | Exist<br>Exist         |
| B       | 2                      | x <sub>1</sub> x <sub>2</sub> x <sub>3</sub><br>y <sub>1</sub> y <sub>2</sub> y <sub>3</sub><br>uv ( $\pm 15^\circ$ ) | PWC           | 3x512<br>2x288,320<br>2x416      | 1.00x0.62                           | 5.1            | Exist<br>Exist<br>E557 |
| C       | 2                      | x,y<br>u ( $15^\circ$ )   | PWC           | 512,320<br>416                   | 1.00x0.62                           | 6.6            | Exist<br>E557          |
| D       | 2                      | x <sub>1</sub> x <sub>2</sub><br>uv ( $\pm 15^\circ$ )  | PWC           | 2x992<br>2x864                   | 1.93x0.96                           | 8.8            | Exist                  |
|         | 3                      | y <sub>1</sub> y <sub>2</sub>   |               | 2x320                            |                                     |                | Exist                  |
|         | 1                      | x <sub>3</sub> x <sub>4</sub>   |               | 2x320                            | 0.32x0.32                           |                | E557                   |
| DR      | 19                     | x <sub>1</sub> x <sub>1</sub> '<br>uv ( $\pm 15^\circ$ )<br>x <sub>2</sub> x <sub>2</sub> '<br>uv ( $\pm 15^\circ$ )  | Drift         | 2x176<br>2x192<br>2x176<br>2x192 | 3.34x1.68                           | 12.8           | Exist<br>Exist         |
| E       | 2.5                    | x <sub>1</sub> x <sub>2</sub> y <sub>1</sub> y <sub>2</sub>   | PWC           | 4x800                            | 2.00x2.00                           | 13.4           | E557                   |
| F       | 2                      | xyuv ( $\pm 45^\circ$ )   | PWC           | 4x320                            | 0.62x0.62                           | 13.7           | Exist                  |
| G       | 4.6                    | xx'yy'  | PWC           | 4x320                            | 1.48x1.48                           | 26.2           | E557                   |

\*Prime indicates planes staggered by half-wire spacing. x planes measure charge particle coordinates in the bend plane.

\*\*For comparison the magnet apertures downstream are: M1(.61x.36 m<sup>2</sup> at 3.9 m), M2(1.22x.72 m<sup>2</sup> at 8.5 m).

Note that the  $\gamma$ -chamber is not listed as it is discussed in the text.

TABLE III. Gas Cherenkov Thresholds (GeV/c)

| <u>Quantity/Gas:</u>   | <u>He</u> | <u>Ne</u> | <u>N<sub>2</sub></u> | <u>.8He-.2N<sub>2</sub></u> |
|------------------------|-----------|-----------|----------------------|-----------------------------|
| n                      | 1.000035  | 1.000067  | 1.000300             | 1.000084                    |
| P( $\pi$ )             | 16.7      | 12.0      | 5.7                  | 10.8                        |
| P(K)                   | 59.4      | 42.8      | 20.2                 | 38.7                        |
| P(p)                   | 112.6     | 81.0      | 38.3                 | 73.4                        |
| $\theta_{mr}(\beta=1)$ | 8.4       | 11.6      | 24.5                 | 12.9                        |

TABLE IV. Spectrum Aperatures in mr Assuming 100% Efficiency

| <u>Coordinate Plane</u> | <u>Momentum (GeV/c)</u>   | <u>DEVICE</u>    |                      |                  |                      |
|-------------------------|---|------------------|----------------------|------------------|----------------------|
|                         |   | <u>A Station</u> | <u>M1 Downstream</u> | <u>C Station</u> | <u>M2 Downstream</u> |
| Vertical                | any   | $\pm 72$         | $\pm 46$             | $\pm 46$         | $\pm 42$             |
| Horizontal              | $\infty$  | $\pm 72$         | $\pm 78$             | $\pm 76$         | $\pm 72$             |
|                         | 100   | $\pm 72$         | $\pm 77$             | $\pm 72$         | $\pm 66$             |
|                         | 50  | $\pm 72$         | $\pm 75$             | $\pm 68$         | $\pm 61$             |
|                         | 25  | $\pm 72$         | $\pm 72$             | $\pm 61$         | $\pm 50$             |
|                         | $11.5 \left\{ \begin{array}{l} \text{kaon} \\ x_F=0 \end{array} \right\}$ | $\pm 72$         | $\pm 65$             | $\pm 44$         | $\pm 25$             |

TABLE V. Trigger Summary

| <u>Idealized Trigger</u> <sup>1</sup> | <u>Possible State</u> | <u>Branching Fractions</u> <sup>2</sup> |
|---------------------------------------|-----------------------|---|
| $1K_S^0 2K^\pm$                       | $D_0^+ F^\pm$         | 0.028                                   |
|                                       | $D F^\pm$             | 0.020                                   |
| $3K^\pm$                              | $D_0^+ F^\pm$         | 0.030                                   |
|                                       | $D F^\pm$             | 0.065                                   |
| $4K_S^0$                              | $F^+ F^-$             | 0.002                                   |
| $3K_S^\pm 1K^\pm$                     | $F^+ F^-$             | 0.016                                   |
| $2K_S^\pm 2K^\pm$                     | $F^+ F^-$             | 0.047                                   |
| $1K_S^\pm 3K^\pm$                     | $F^+ F^-$             | 0.063                                   |
| $4K^\pm$                              | $F^+ F^-$             | 0.021                                   |
| $(K^+ K^-) (K^+ K^-)$                 | $\phi\phi$            | 0.240                                   |

---

<sup>1</sup>The actual trigger criteria will be set more stringently as discussed in the text. Within the less stringent triggers will exist events in which some of the kaons were not detected in the apparatus weighted by the combinatorics. <sup>2</sup>Assume half of the Fs decay into 2 kaons and charge symmetry.

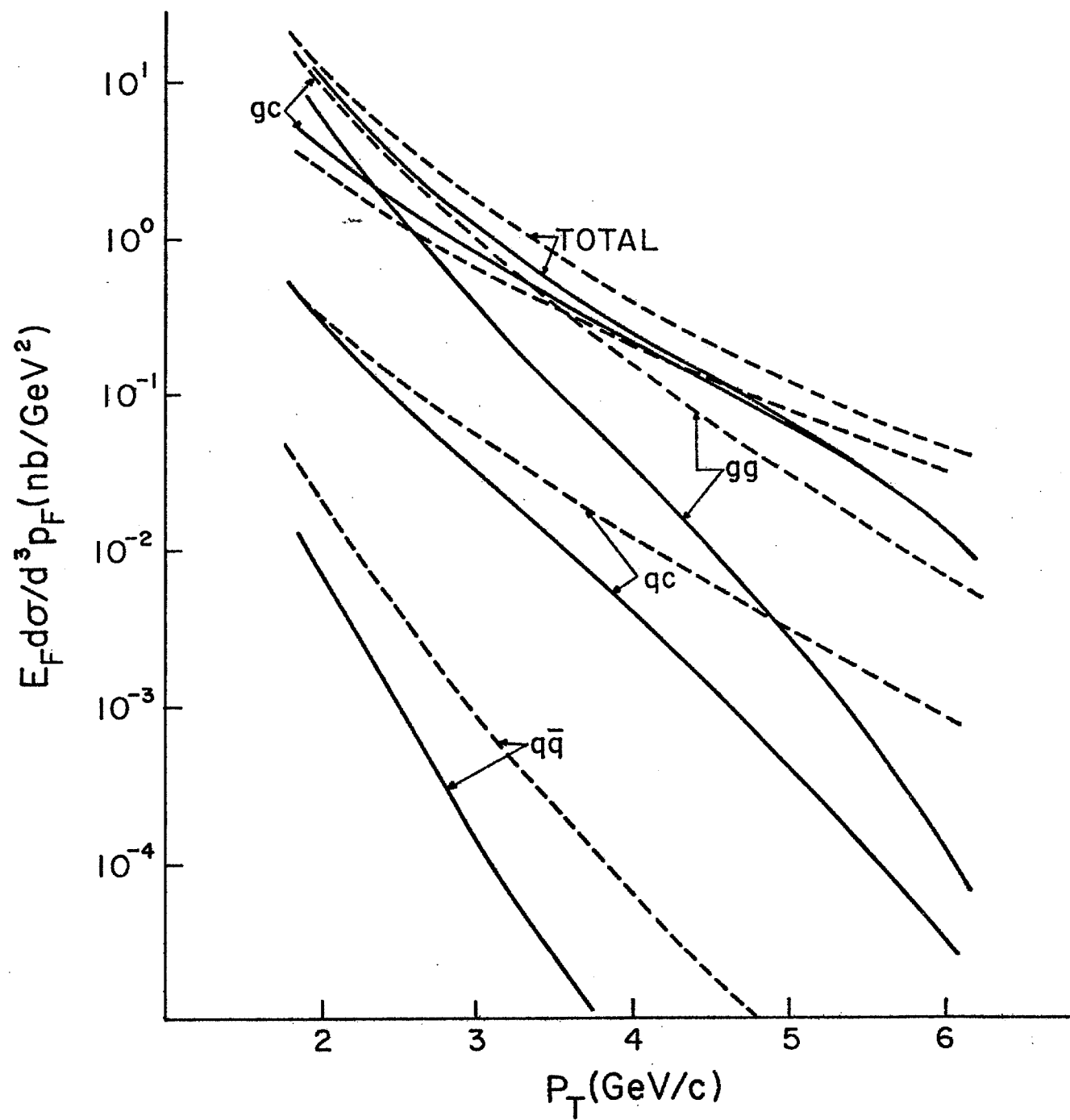


Fig. 1



Fig. 2 Experimental Layout

